



Limettin and PD98059 Mitigated Alzheimer's Disease Like Pathology Induced by Streptozotocin in Mouse Model: Role of *p*-ERK1/2/*p*-GSK-3 β /*p*-CREB/BDNF Pathway

Rofida M. Hassan¹ · Nesrine S. Elsayed² · Naglaa Assaf¹ · Barbara Budzyńska³ · Krystyna Skalicka-Woźniak⁴ · Sherehan M. Ibrahim^{2,5}

Received: 13 December 2024 / Accepted: 27 April 2025

© The Author(s) 2025

Abstract

Sporadic Alzheimer's disease (SAD) represents one of the major memory deficits that is characterized by tau hyperphosphorylation and amyloid beta (A β) deposition in the brain. Both are considered AD hallmarks which are mediated through neuroinflammation, oxidative stress, and cholinergic circuit interruption. This study aimed to show how limettin and PD98059 exert a neuroprotective effect against SAD and the possible role of the extracellular regulated kinase (*p*-ERK1/2) and glycogen synthase kinase-3 beta (*p*-GSK-3 β) (Ser9)/cAMP-response element binding protein (*p*-CREB) (Ser133)/brain derived neurotrophic factor (BDNF) pathway. Control animals (Group I) received the vehicles, group II received PD98059 (10 mg/kg/i.p), while group III was administered limettin (15 mg/kg/i.p). Additionally, the other three groups received a single dose of streptozotocin (STZ; 3 mg/kg/ICV), where group IV served as the SAD group, while groups V and VI received PD98059 and limettin daily for 3 weeks, respectively. The SAD animals receiving PD98059 and limettin increased the number of arm entries, % alternations in Y-maze, with reduction in mean escape latency, increase in time spent in target quadrant and platform crossing in Morris Water Maze, compared to the SAD group. Additionally, PD98059 and limettin administration to the STZ group downregulated persistent activation of *p*-ERK1/2 which in turn increased *p*-GSK-3 β (Ser9), leading to enhanced *p*-CREB (Ser133) and BDNF expressions, as well as reducing inflammatory markers *viz.*, nuclear factor-kappa B and interleukin-6, leading to decreased A β deposition. Both treatments reduced immunohistochemical *p*-tau expression, brain edema, and increased intact neuron cells remarkably. Thus, based on these findings, PD98059 and limettin may have promising effects in protecting against SAD. Using blockers/inhibitory molecules are recommended to confirm effect through the corresponding pathway.

Keywords *p*-ERK1/2 · Limettin · Neuroinflammation · PD98059 · Sporadic alzheimer's disease · STZ

✉ Rofida M. Hassan
rofigda.hassan@must.edu.eg

¹ Department of Pharmacology and Toxicology, College of Pharmaceutical Sciences and Drug Manufacturing, Misr University for Science and Technology (MUST), 6th of October city, Giza 12563, Egypt

² Department of Pharmacology and Toxicology, Faculty of Pharmacy, Cairo University, Cairo 11562, Egypt

³ Independent Laboratory of Behavioral Studies, Medical University of Lublin, Lublin 20-093, Poland

⁴ Department of Chemistry of Natural Products, Medical University of Lublin, Lublin 20-093, Poland

⁵ Department of Pharmacology and Toxicology, Faculty of Pharmacy, Modern University for Technology and Information (MTI), Cairo 11571, Egypt

Abbreviations

A β	Amyloid Beta
AChE	Acetylcholinesterase
AD	Alzheimer's Disease
Akt	Protein Kinase B
ANOVA	Analysis of Variance
BACE-1	β -site Amyloid Precursor Protein Cleaving Enzyme 1
BDNF	Brain Derived Neurotrophic Factor
CREB	cAMP-Response Element Binding Protein
DMSO	Dimethyl Sulfoxide
ELISA	Enzyme-Linked Immunosorbent Assay
ERK	Extracellular Regulated Kinase
GSK	Glycogen Synthase Kinase

HRP	Horseradish Peroxidase
ICV	Intracerebroventricular
IL	Interleukin
i.p	Intraperitoneally
LTP	Long Term Potentiation
MAPK	Mitogen Activated Protein Kinase
MEL	Mean Escape Latency
MWM	Morris Water Maze
NF- κ B	Nuclear Factor-Kappa B
p	Phosphorylated
PVDF	Polyvinylidene Fluoride
SAD	Sporadic Alzheimer's Disease
SAP	Spontaneous Alteration Percentage
SDS-PAGE	Sodium Dodecyl Sulphate-Polyacrylamide Gel Electrophoresis
Ser	Serine
STZ	Streptozotocin
TEST	Tris-Buffered Saline with Tween 20 Buffer

Introduction

The most prevalent kind of dementia, primarily affecting the elderly, is Alzheimer's disease (AD) with preferential index to female gender (Zhang et al. 2021). The US population estimate for 2022 shows that the prevalence of sporadic Alzheimer's disease (SAD) is 5.0% among those 65 to 74 years old, 13.1% among those 75 to 84 years old, and 33.2% among those 85 years of age and older (Lane et al. 2022).

People diagnosed with AD displayed cognitive impairment symptoms such as forgetting things, having problems in following conversations, finishing tasks or making decisions as well (Dillon et al. 2013). Furthermore, neuropsychiatric symptoms, such as depression and apathy, were observed and associated to memory decline in mild/early AD, besides verbal and physical agitation (Lyketsos et al. 2011).

It is well known that AD is characterized by neurodegeneration in hippocampal, cortical regions, and occurrence of a cholinergic imbalance stemming from oxidative stress and inflammation in neurons, resulting in excessive tau phosphorylation and aggregation of amyloid beta (A β) in the brain (Kumar et al. 2015). This could be due to reducing α -secretase activity while increasing β -site amyloid precursor protein cleaving enzyme (BACE-1) activity, leading to toxic A β accumulation in addition to neurofibrillary tangles formation (Nistor et al. 2007).

Furthermore, neuroinflammation plays role in AD pathology via the generation of various inflammatory markers such as nuclear factor-kappa B (NF- κ B) which activates interleukin-6 (IL-6) that promotes further release of different pro-inflammatory cytokines resulting in the synthesis

of inflammatory mediators in an endless cycle (Wang et al. 2003). As well, NF- κ B activation is linked to the activation of BACE-1 followed by A β deposition (Tamagno et al. 2012).

Noteworthy, amyloidogenesis is linked to insulin signaling pathway as A β deposition accompanied by disrupting expression of some mediators, resulting in insulin receptor desensitization (Folch et al. 2018). Likewise, it was reported that insulin receptors are downregulated in AD patients to point the function of insulin signaling in memory deterioration (Burillo et al. 2021), this relation was approved via enhancing the release of acetylcholine in brain through intracerebroventricular (ICV) administration of insulin (Agrawal et al. 2008).

Moreover, glycogen synthase kinase-3 beta (GSK-3 β) has been considered to play an important role in the pathogenesis of type 2 Diabetes Mellitus and AD, where it acts as "tau-kinase I" that contribute to the phosphorylation of tau protein in AD (Hoppe et al. 2010). Phosphorylation of GSK-3 β at Ser9 inhibits its kinase activity (Fang et al. 2000; Giese 2009) thus enhancing long term potentiation (LTP) which represents a form of flexibility and adaptation of synapse that underlies memory formation (Tang et al. 2014). On the other hand, active p-GSK-3 β (Tyr216) co-localizes with neurofibrillary tangles and enhance generation of the harmful A β 42/40 in AD (Amaral et al. 2021).

Remarkably, GSK-3 β when exposed to A β , may suppress the phosphorylation of the cAMP-response element binding protein (CREB) more strongly, thus brain derived neurotrophic factor (BDNF) down regulation. Such molecule acts as an encouraging modifier of several types of neural plasticity in the nervous system of adults (Tang et al. 2014).

Currently in this work, ICV injection of streptozotocin (STZ), a natural compound isolated from *Streptomyces achromogenes*, in sub-diabetogenic doses of STZ (1–3 mg/kg) (Grieb 2016) has been activated microglial cells, which released large quantities of free radicals and cytokines that cause harm to neurons. (Chen et al. 2020). Besides, in accordance to previous literature, tau hyperphosphorylation and A β generation, as well as GSK- α and β activation, are related to STZ-induced insulin receptor desensitization. (Rajasekar et al. 2014). Likewise, Animals treated with ICV-STZ also showed a loss in their ability to learn and remember things, suggesting cholinergic dysfunction brought on by low acetylcholine levels. (Saria et al. 2015). Consequentially, because STZ model displays numerous behavioral, neurochemical, and structural alterations that are similar to those seen in human SAD, it is regarded as a widely recognized representative model of SAD (Kamat 2015; Mullins et al. 2017).

The current mainstays in Alzheimer's therapy are donepezil and galantamine, acetylcholinesterase (AChE)

inhibitors, that improve cognitive and behavioral symptoms in mild to moderate AD (Zec and Burkett 2008). Additionally, memantine, an N-methyl-D-aspartate receptor antagonist, had been accepted for management of more advanced and severe cases of the disease (Olivares et al. 2013).

Unfortunately, several side effects are observed such as nausea, vomiting, loss of appetite, muscle cramps, and diarrhea through using AchE inhibitors. Besides, dizziness, constipation, headache, and shortness of breath were reported with memantine administration. Additionally, there are serious side effects seen with anti-amyloid drugs such as aducanumab, an anti-amyloid antibody, that is taken intravenously every month, like headache, falls, and amyloid-related imaging abnormalities which is a temporary swelling with or without spots of bleeding in areas of the brain specially in ApoE ϵ 4 gene carriers (Kataria 2021; Honig et al. 2023). Therefore, efforts have been done to nominate new treatments targeting different pathways with few or no side effects for enhancing fulfillment and quality patient's life compliance.

PD98059, a mitogen activated protein kinase MAPK (MEK) specific inhibitor, shows promising effect against neurodegeneration through preventing the phosphorylation of tau triggered by A β (Rapoport and Ferreira 2000). PD98059 has been also found to have many beneficial effects in certain diseases such as neuropathy as it potentiates morphine analgesia by inhibiting levels of MAPK, NF- κ B, IL-6, and enhancing anti-nociceptive IL-10 factor (Rojewska et al. 2015). Moreover, PD98059 also shields from neuronal cell destruction caused by oxidative damage in oligodendroglia cell line (Subramaniam and Unsicker 2010).

Limettin (5,7-dimethoxycoumarin), citropten, is found in bergamot oil and it is a derivative of coumarins which are abundant metabolites present in extracts from many plant families, including the Rutaceae and Asteraceae (Epifano et al. 2009). It displayed anti-inflammatory and antioxidant (Kostova et al. 2012; Seong et al. 2019; Kowalczyk et al. 2022a; Lee et al. 2022a) via hindering nitrite, prostaglandin E2, IL-6, and tumor necrosis factor- α in addition to upregulation of expression of the cytoprotective heme oxygenase-1 enzyme (Yu et al. 2005; Pan et al. 2010).

Likewise, aromatic ring of coumarins can attach to AchE, thereby blocking the development of A β -AchE conjugates as well as possessing BACE-1 inhibiting activity in comply with an in vitro study that discussed the potential of coumarins to combat against AD focusing on the structure-activity analysis (Ali et al. 2016), so it may show promising effect against AD. This work aimed to assess the effect of limettin, as a type of furanocoumarin in amelioration of

SAD and its role in modulation of *p*-ERK1/2/*p*-GSK-3 β /*p*-CREB/BDNF pathway and associated neuroinflammation using PD98059.

Materials and Methods

Ethical Statement

Methods and procedures were followed throughout this work using US National Institutes of Health guidelines for the treatment and care of laboratory animals (NIH publication No. 85–23, revised 2011). The Research Ethics Committee had approved these procedures for use in experimental studies at the Faculty of Pharmacy, Cairo University, Cairo, Egypt, under number of permissions PT-(3020).

Animals

Three to four months old, adult male mice weighing 25 to 30 g were acquired from the Faculty of Veterinary Medicine Cairo University (Giza, Egypt). They have been adapted to normal housing circumstances with a 12-hour cycle of light and dark at room temperature 24–26 °C and 60% relative humidity. Food and water were provided on a free-for-all basis.

Chemicals

STZ, limettin, and PD98059, the ERK1/2 inhibitor, had been obtained from Sigma–Aldrich (Missouri, USA). STZ was dissolved in saline, while limettin, and PD98059 were dissolved in 1% dimethyl sulfoxide (DMSO). Further analytical-grade compounds had been bought from reputable commercial vendors. Pilot study was established for limettin dose selection (Supplementary material)(Lee et al. 2022a), while other doses were used according to the previous literatures (Di Paola et al. 2010; Grieb 2016).

SAD Induction

Thiopental (30 mg/kg/i.p) was utilized to anesthetize the mice (Gargiulo et al. 2012). Then, STZ was injected at a dose of 3 mg/kg/ICV (Grieb 2016) using the free hand technique. The bregma could be identified by visualizing an equilateral triangle between the eyes and the center of the skull, then, the needle was inserted directly through the skin and skull into the lateral ventricle, 1 mm lateral to bregma after using downward pressure above the ears (Fronza et al. 2019; Sirwi et al. 2021).

Experiment Design

Animals have been randomized, divided into 6 groups and every group contained 12 mice (6 in each cage) as follows: Group I (Control group) injected normal saline via ICV route followed by intraperitoneal (i.p) 1% DMSO injection for 3 weeks and considered as the control group, while animals in groups II (PD98059 group) and III (limettin group) received PD98059 (10 mg/kg; i.p) (Di Paola et al. 2010) and limettin (15 mg/kg; i.p), respectively after single ICV saline injection and continued for 3 weeks. Moreover, mice in group IV (STZ group) were administered ICV- STZ (3 mg/kg) (Grieb 2016) as a single dose and serves as the model group. Furthermore, group V (STZ+PD98059 group) and VI (STZ+limettin group) received PD98059 (10 mg/kg/day; i.p) and limettin (15 mg/kg/day; i.p), respectively for 3 weeks, 24 h after single STZ injection (Rajkumar et al. 2022). The experimental design was illustrated in Fig. 1.

Tissue Sampling

After 24 h of last dosing, Y-Maze and Morris Water Maze were accomplished, then animals were euthanized using cervical dislocation under an overdose of thiopental anesthesia. The whole brain ($n=3$ /group) has been preserved in 10% formalin for histopathology and immunohistochemical investigation. Hippocampus of the remaining animals were isolated and stored in -80°C to assess A β , NF- κ B, IL-6,

BACE-1, and BDNF by enzyme-linked immunosorbent assay (ELISA) ($n=6$ /group), while relative protein expression of p -ERK1/2, p -GSK-3 β (Ser9), and p -CREB (Ser133) were measured by Western Blot ($n=3$ /group).

Assessed Parameters

Behavioural Test

Y-Maze Test Y-maze examination assesses temporary memory (short term) (Cognato et al. 2012) and the current study utilized a three-armed, Y-shaped maze made of wood. Every single arm extended from a central platform at a 120° angle with a length of 35 cm, height of 25 cm, and width of 10 cm. Rather than exploring the well-known arm of the maze, normal animals would rather explore a new one. Two days in a row were used to conduct the test (Rasheed et al. 2018). Every mouse was placed on the platform and given free movement for ten minutes to explore the maze on the first day, which was set aside for training. On test day, a record of every mouse's arm entry sequence was kept for the 10-minute session. Following each mouse, 70% ethanol was used to clear the maze from any smell cues that would cause inaccurate assessment.

The consecutive entrance into every single arm of the three in the form of overlapping triad groups was recorded as an actual alternation. Possible alternations could be

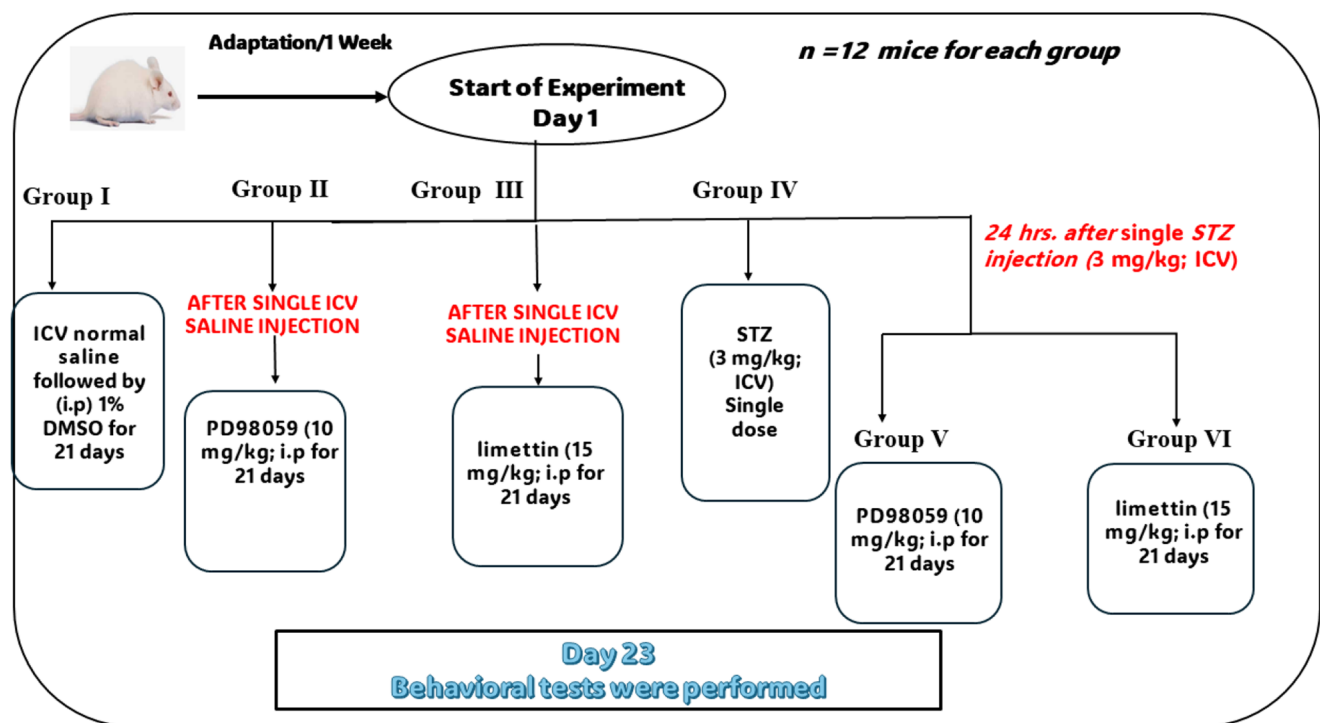


Fig. 1 Experimental design

expressed as the overall arm entries-2 (Prieur and Jadavji 2019; Rattanapornsompong et al. 2019).

Possible Alternations=overall arm entries-2.

The spontaneous alternation percentage (SAP) was computed through dividing actual alternations by possible alternations then multiply the result by 100.

% Alternations= (Actual alternations)/ (Possible alternations) \times 100.

Morris Water Maze (MWM) The MWM evaluates a small rodent's visual-spatial and visual-short-term memory skills (D'Hooge and De Deyn 2001). In the current investigation, a stainless-steel circular pool with a non-reflective internal surface having 120 cm circumference and 51 cm elevation—has been employed. With the assistance of 2 vertical strings that were fixed to the pool's edge, The pool's aqua level was only half of its height, the same as ambient temperature and was randomly split into four sections/ quadrants of equal size. Within the pool's target quadrant, an immersed 10 cm in width and 28 cm in height platform has been positioned 1 cm under the aqua's surface. Throughout the test, the platform stayed in its original position. To make the water opaque, non-toxic green dye was applied to render the platform undetectable.

In normal circumstances, animals gain up the skill of swimming straight toward the platform and arriving there faster. This procedure was carried out over the course of five days as each mouse was subjected to two successive trials on the first 4 days of the test, with an interval of at least 15 min between the trials. The maximum time for each trial was 120 s. If the mouse found the hidden platform within the 120 s, it was kept there for an additional 20 s and then removed. The mouse that failed to find the hidden platform during the designated time was gently guided onto the platform and kept there for 20 s (D'Hooge and De Deyn 2001; Vorhees and Williams 2006). On the fifth day, the probe-trial session, the platform was eliminated from the pool and the mice were given sixty seconds to explore it. The mean escape latency (MEL) on the training days and on the test day as well as the time spent in the target quadrant—where the hidden platform had been—and number of platform crossing were noted as markers of retrieval or memory (Nunez 2008).

Estimation of Biochemical Parameters

Mouse ELISA kits were acquired from My Bio Source, San Diego, CA, USA to assess hippocampal content of A β , NF- κ B, IL-6, BACE-1, and BDNF (Cat No. MBS265825, MBS043224, MBS824703, MBS7234786, and MBS355435), respectively. Protein content was estimated

using Bradford method (Marshall and Williams 1993). A β , NF- κ B, IL-6, and BDNF were expressed as (pg/mg protein) while BACE-1 (ng/mg protein). Every step of the process was carried out as directed by the manufacturer.

Western Blot Analysis

Hippocampal protein expression of *p*-ERK1/2, *p*-GSK-3 β (Ser9), and *p*-CREB (Ser133) were assessed. In brief, RIPA lysis buffer PL005, obtained from Bio BASIC INC. (Marham Ontario L3R 8T4 Canada) was used for hippocampal protein extraction. The second step is sample separation on sodium dodecyl sulfate poly acrylamide gel electrophoresis (SDS-PAGE), which isolates proteins according to their molecular weight. After that, protein bands have been relocated to polyvinylidene fluoride (PVDF) membrane using BioRad Trans-Blot Turbo instrument. For one hour at ambient temperature, the membrane was soaked in tris-buffered saline containing 3% bovine serum albumin and Tween 20 buffer to prevent signal interference arising from non-specific interactions between the corresponding antibodies and the PVDF membrane. Incubation of the blotted target protein was done at four degrees Celsius all night with primary polyclonal antibody for *p*-ERK1/2 (Catalog No: 44-654G), *p*-GSK-3 β (Ser9) (Catalog No: PA5-104555), and *p*-CREB (Catalog No: PA1-4619) obtained from Thermo Fisher Scientific Inc. (MA, USA). Incubation was done within horseradish peroxidase (HRP)-conjugated secondary antibody (Goat anti rabbit IgG- HRP- Goat mab -Novus Biologicals) solution over 60 min at room temperature in contrast to the blotted target protein. Finally, by utilizing stain-free technology and ChemiDoc TM imager, the acquired band magnitude has been normalized to β -actin and then viewed. Unspecified arbitrary units were used to define the values.

Histopathological Examination

Samples of mouse brain tissue were preserved for 72 h in 10% neutral buffered formalin, then processed through successive ethanol grades, cleaned in xylene, and inserted into paraplast tissue embedding media (Leica Biosystems). Longitudinal parts of brain ordered in serial sets (4 μ m thick) have been prepared to demonstrate hippocampal CA3 regions through Hematoxylin and Eosin staining to assess neuronal damage, brain matrix edema, and glial cell infiltrates. Toluidine blue staining was applied to assess the mean intact neurons count neurodegeneration (Yong 1992). Focusing on CA3, as CA3 region is important for retrieving stored information based on certain cues such as recognizing certain features of the surrounding environment while the CA1 region plays a role in integration of received information mainly, and the subiculum of CA1 contributes

to memory (Valenzuela and Morton 2014; Schlichting et al. 2014). Furthermore, the CA3 region has specific attention in recent years due to its involvement in memory processes, susceptibility to seizures and neuro-degeneration and the CA3 subsection has a higher degree of neuronal connection compared to other hippocampus sections (Cherubini and Miles 2015; El Tabaa et al. 2022; Rui et al. 2025). Also, upon our microscopic inspection, the CA3 region was clearly affected, and no observation was found on CA1 region.

Immunohistochemistry

A five-micron tissue segment immersed in paraffin has been prepared. The manufacturer's procedure was followed throughout the immunohistochemistry testing. Brain segments have been kept with anti-*p*-tau antibody (1:100–thermofisher scientific, MA, USA, Cat. No. 44-742G) overnight at 4 °C then, for 20 min, with HRP as the secondary antibody (Envision kit DAKO), afterwards, hippocampus CA3 region of every specimen was randomly chosen, and 6 non-interconnected fields were imaged to determine the area % of *p*-tau (Abbas et al. 2021). The pyramidal neurons layer of hippocampus CA3 zone was used for immunohistochemical quantification.

Statistical Analysis

Analysis of data has been conducted using GraphPad Prism (VER 10.4.1) program, results were represented as mean \pm SD through one-way analysis of variance (ANOVA) followed by Tukey's multiple comparison test. Level of significance was applied at $p < 0.05$. However, a two-way ANOVA with Tukey's multiple comparisons tests were

utilized to analyze the learning performance for 4 days in the MWM trial in mean escape latency (MEL). Moreover, to compare the histopathological scoring, the Kruskal-Wallis's test followed by Dunn's post hoc test for multiple comparison was used.

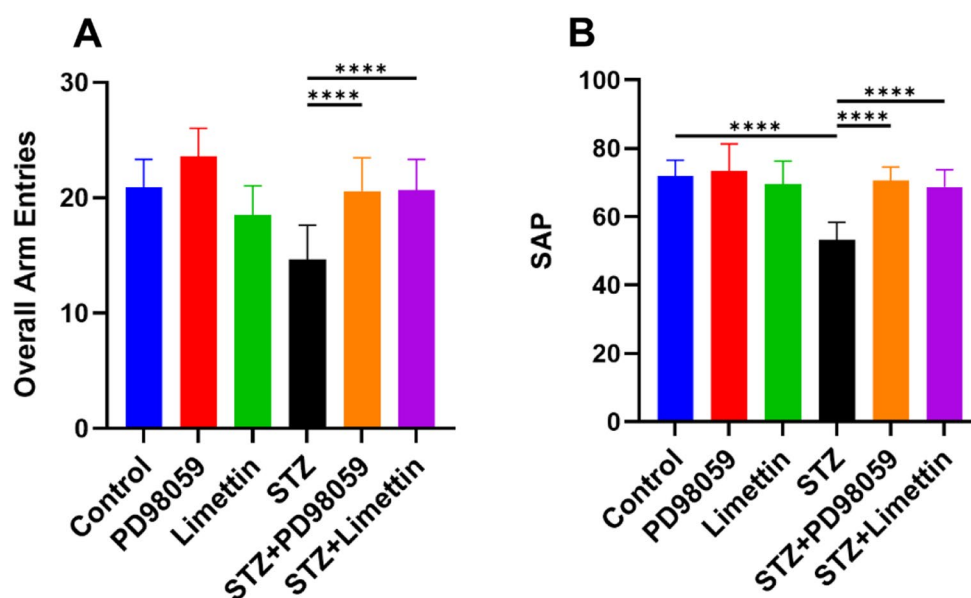
Results

The findings showed that there was no significant difference between control, PD98059, and limettin groups, therefore the model and treated groups were compared to the control group.

Effect of PD98059 and Limettin on Y-Maze Overall Arm Entries and SAP in SAD Mice Model

The STZ injected mice exhibited lowering in the overall number of entries into each arm (Fig. 2A) as well as SAP (Fig. 2B) to 70% (14.62 ± 2.93 ; $p < 0.0001$) and 74% (53.19 ± 5.17 ; $p < 0.0001$), respectively, in comparison with control animals, while in the STZ+PD98059 and STZ+limettin groups, the overall number of entries into each arm is increased by 40% for both (20.58 ± 2.88 ; $p < 0.0001$; STZ+PD98059) (20.67 ± 2.67 ; $p < 0.0001$; STZ+limettin), while SAP elevated by 33% (70.54 ± 3.97 ; $p < 0.0001$) and 30% (68.68 ± 4.99 ; $p < 0.0001$), respectively, as compared to STZ model mice. Thus, PD98059 and limettin lessened the short-term memory impairment caused by STZ.

Fig. 2 Effect of PD98059 and limettin on Y-maze overall arm entries and SAP in SAD mice model. PD98059 (10 mg/kg; i.p) and limettin (15 mg/kg; i.p) had been provided during a 21-day period post single ICV-STZ injection-induced SAD in mice. Data is set as mean \pm SD; ($n = 12$), the asterisks (****) is statically significant at $p < 0.0001$, tested through Tukey's multiple comparisons following One Way ANOVA. ANOVA: Analysis of variance, SAD: Sporadic Alzheimer disease, SAP: Spontaneous alteration percentage; STZ: Streptozotocin



Effect of PD98059 and Limettin on MWM Mean Escape Latency (MEL), the time Spent in the Target Quadrant, and Platform Crossing in SAD Mice Model

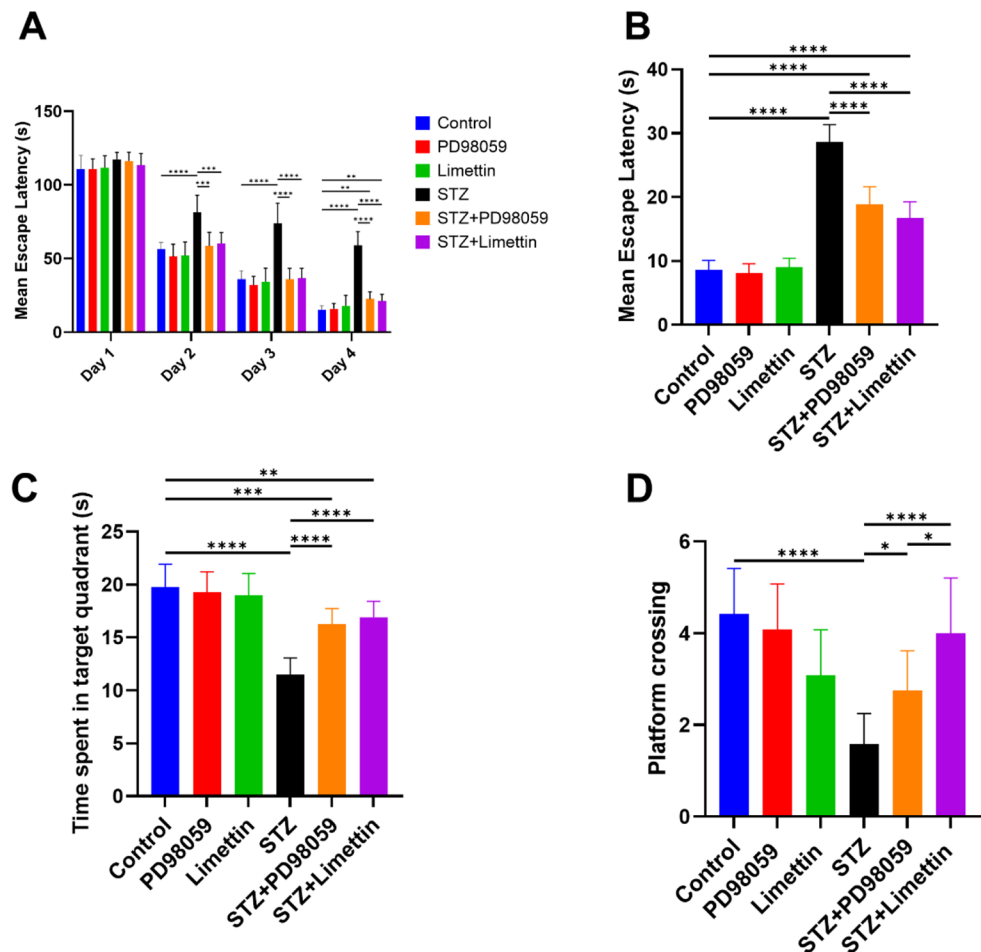
On training days, MEL was measured and all groups showed no significant difference on the first day, while there was significant improvement in learning and memory on 2nd, 3rd, 4th day in PD98059 and limettin treated mice, compared to STZ group (Fig. 3A). On the test day, the model group increased the MEL (Fig. 3B) by 234% (28.67 ± 2.67 ; $p < 0.0001$), in comparison with control group. Notably, PD98059 and limettin treated mice displayed significant MEL reduction compared to STZ model group by 35% (18.83 ± 2.79 ; $p < 0.0001$) and 42% (16.75 ± 2.53 ; $p < 0.0001$), respectively. Moreover, STZ model group revealed significant decline in the time spent in the target quadrant (Fig. 3C) in comparison with control animals by 41% (11.50 ± 1.57 ; $p < 0.0001$), while PD98059 and limettin treated groups showed marked rise in the time spent in the target quadrant, in comparison with STZ model group by 41% (16.25 ± 1.49 ; $p < 0.0001$) and 48% (16.92 ± 1.51 ; $p < 0.0001$) respectively. STZ also decreased the number of platform crossing (Fig. 3D) significantly by 64% (1.58 ± 0.67 ; $p < 0.0001$), as compared

to the control animals, while both PD98059 and limettin treated groups showed marked increase in platform crossing by 74% (2.750 ± 0.87 ; $p < 0.05$) and 153% (4.00 ± 1.21 ; $p < 0.0001$), respectively as compared to model group. Additionally, limettin treated group showed significant increase in platform crossing more than PD98059 by 46% (4.00 ± 1.21 ; $p < 0.05$).

Effect of PD98059 and Limettin on *p*-ERK1/2, *p*-GSK-3 β (Ser9), *p*-CREB(Ser133) Expression, as Well as BDNF Hippocampal Content in SAD Mice Model

The expression of *p*-ERK1/2 (Fig. 4A) was upregulated to 6.4-folds (6.58 ± 1.85 ; $p < 0.0001$) while *p*-GSK-3 β (Ser9) (Fig. 4B) is downregulated to 22% (0.23 ± 0.06 ; $p < 0.0001$) within model animals, as compared to the control group. The STZ+PD98059 and STZ+limettin groups downregulated *p*-ERK1/2 expression to 47% (3.12 ± 0.83 ; $p < 0.01$) and 44% (2.9 ± 0.80 ; $p < 0.01$), while both treatments upregulated *p*-GSK-3 β (Ser9) by 2.4 folds (0.79 ± 0.09 ; $p < 0.0001$; STZ+PD98059), (0.79 ± 0.15 ; $p < 0.0001$; STZ+limettin), as compared to the model group. Both *p*-CREB (Ser133) expression (Fig. 4C) and BDNF content (Fig. 4D) were

Fig. 3 Effect of PD98059 and limettin on MWM (A) Mean escape latency (MEL) on trial days, (B) MEL on the test day, (C) time spent in the target quadrant, and (D) platform crossing in SAD mice model. PD98059 (10 mg/kg; i.p) and limettin (15 mg/kg; i.p) had been provided during a 21-day period post single ICV-STZ injection-induced SAD in mice. Data is set as mean \pm SD; ($n = 12$), the asterisks (****) show statistical significance at $p < 0.0001$, (***) at $p < 0.001$, (**) at $p < 0.01$ and (*) at $p < 0.05$, tested through Tukey's multiple comparisons following One Way ANOVA. However, a two-way ANOVA with Tukey's multiple comparisons test was utilized to analyze MEL in training days. ANOVA: Analysis of variance, MEL: Mean escape latency, MWM: Morris water maze, SAD: Sporadic Alzheimer's disease, STZ: Streptozotocin



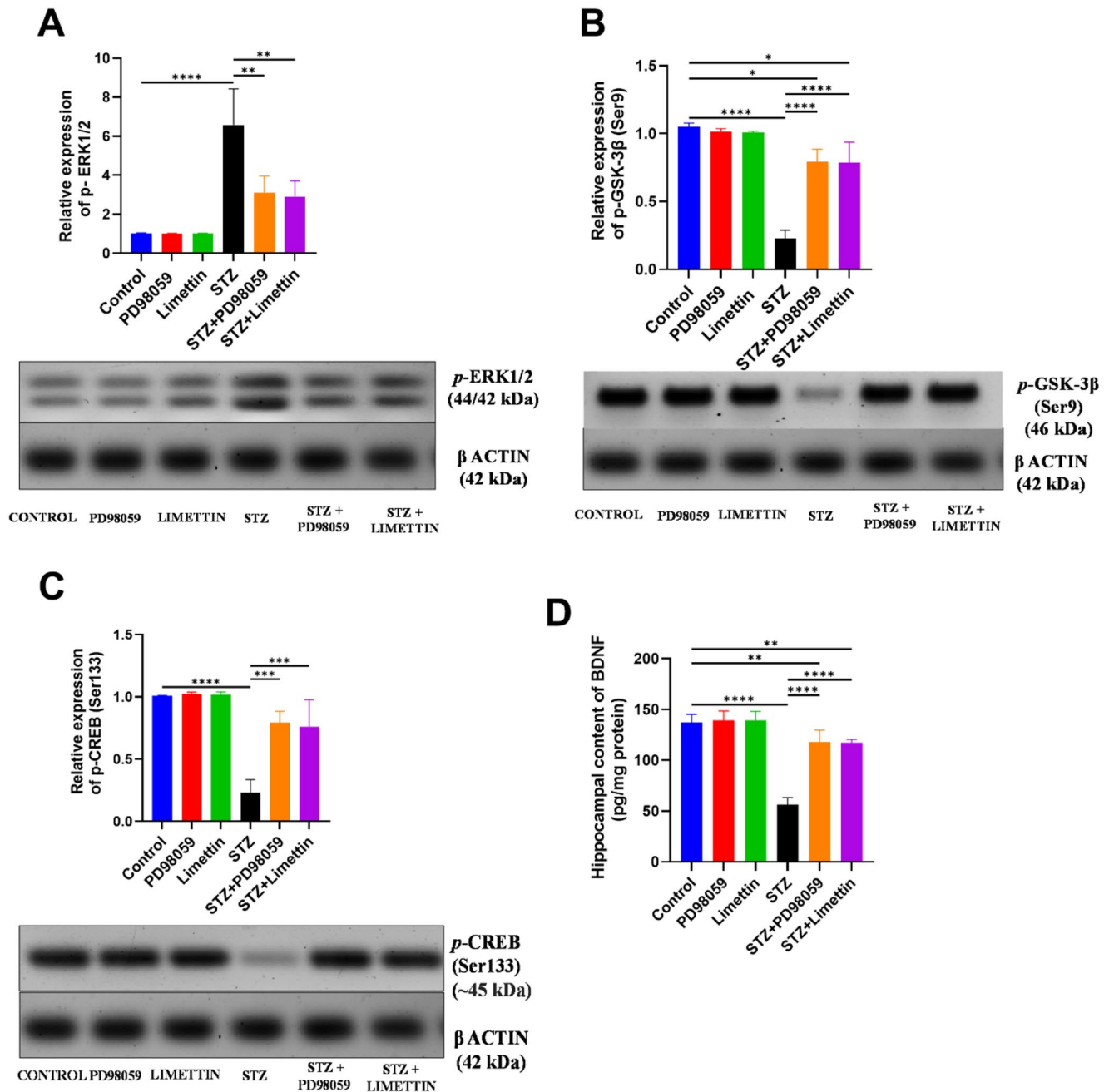


Fig. 4 Effect of PD98059 and limettin on hippocampal content of (A) *p*-ERK1/2, (B) *p*-GSK-3β (Ser9), (C) *p*-CREB (Ser133) expressions, and (D) BDNF and their corresponding blots in SAD mice model. PD98059 (10 mg/kg; i.p) and limettin (15 mg/kg; i.p) had been provided during a 21-day period post single ICV-STZ injection-induced SAD in mice. Data is set as mean ± SD; ($n=3-6$), the asterisks (****) show statistical significance at $p<0.0001$, (***) at $p<0.001$, (**) at

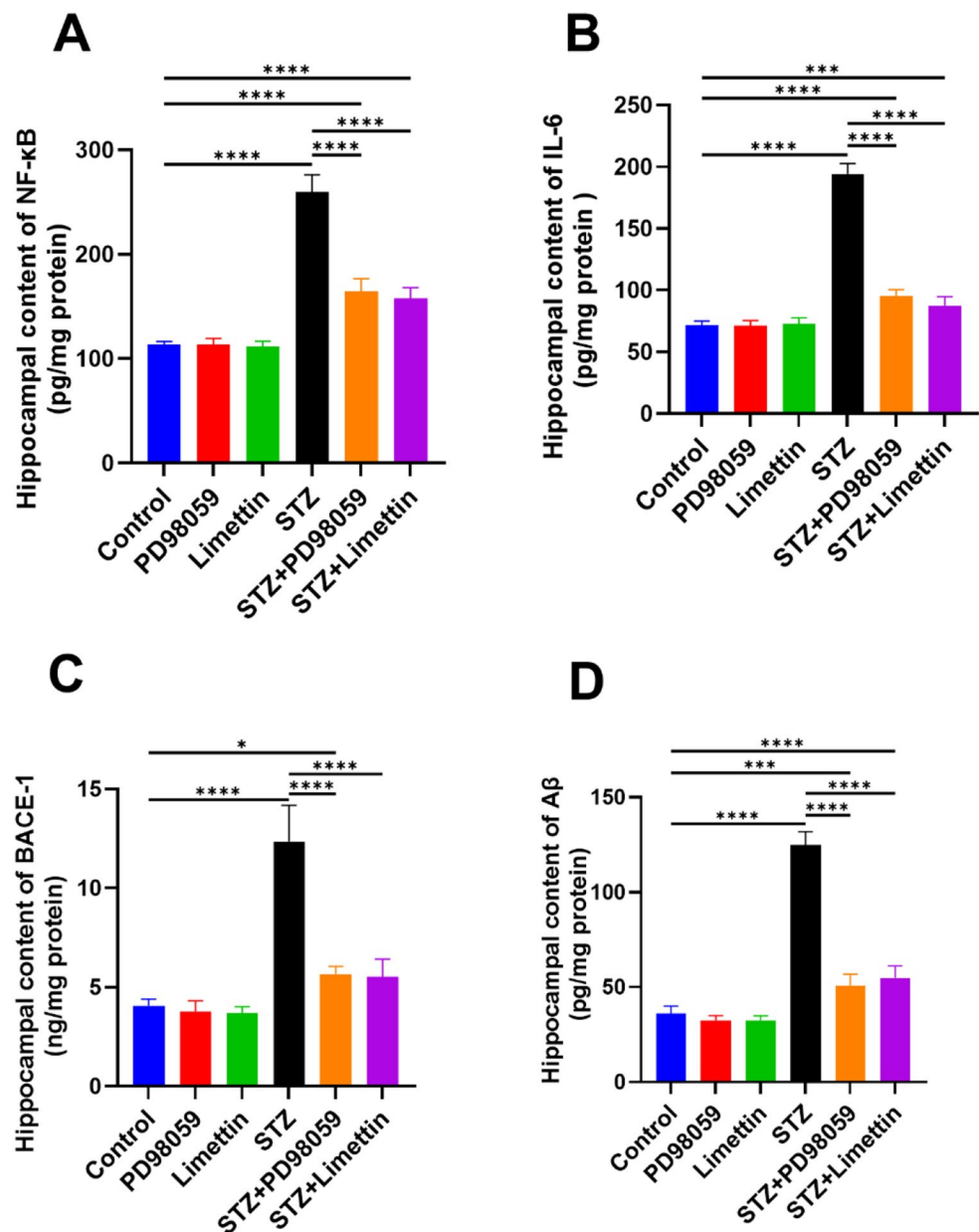
$p<0.01$ and (*) at $p<0.05$, tested through Tukey's multiple comparisons following One Way ANOVA. ANOVA: Analysis of variance, BDNF: Brain derived neurotrophic factor, CREB: cAMP-response element binding protein, ERK1/2: Extracellular regulated kinase, GSK-3β: Glycogen synthase kinase-3 beta, SAD: Sporadic Alzheimer's disease, STZ: Streptozotocin

decreased throughout the model animals to 23% (0.23 ± 0.10 ; $p < 0.0001$) and 41% (56.32 ± 6.91 ; $p < 0.0001$), respectively, compared to the healthy mice. In STZ+PD98059 group, *p*-CREB (Ser133) and BDNF increased by 240% (0.79 ± 0.09 ; $p < 0.001$) and 109% (117.7 ± 12.03 ; $p < 0.0001$), respectively, while the STZ+limettin group stimulated these molecules by 230% (0.76 ± 0.22 ; $p < 0.001$) and 108% (117.4 ± 2.90 ; $p < 0.0001$), respectively, in comparison with STZ-induced SAD mice.

Effect of PD98059 and Limettin on STZ-induced Neuroinflammation and A β Deposition Related Markers in SAD Mice Model

The ICV-STZ group enhanced NF- κ B (Fig. 5A), IL-6 (Fig. 5B), BACE-1 (Fig. 5C), and A β (Fig. 5D) by 129% (259.3 ± 16.85 ; $p < 0.0001$), 170% (194.1 ± 8.45 ; $p < 0.0001$), 203% (12.35 ± 1.83 ; $p < 0.0001$) and 247% (124.7 ± 7.19 ; $p < 0.0001$), respectively, as compared to the control group. The STZ+PD98059 group reduced NF- κ B, IL-6, BACE-1, and A β by 37% (164.1 ± 12.47 ; $p < 0.0001$), 51% (95.56 ± 4.93 ; $p < 0.0001$), 52.5% (5.67 ± 0.39 ; $p < 0.0001$), and 59% (50.88 ± 5.98 ; $p < 0.0001$), respectively, while the STZ+limettin group decreased them by 39%

Fig. 5 Effect of PD98059 and limettin on hippocampal content of (A)NF- κ B, (B) IL-6, (C) BACE-1, and (D) A β in SAD mice model. PD98059 (10 mg/kg; i.p) and limettin (15 mg/kg; i.p) had been provided during a 21-day period post single ICV-STZ injection-induced SAD in mice. Data is set as mean \pm SD; ($n=6$), the asterisks (****) show statistical significance at $p < 0.0001$, (***) at $p < 0.001$, and (*) at $p < 0.05$, tested through Tukey's multiple comparisons following One Way ANOVA. A β : Amyloid beta, ANOVA: Analysis of variance, BACE-1; β -site amyloid precursor protein cleaving enzyme 1, IL-6: Interleukin 6, NF- κ B: Nuclear factor-kappa B, SAD: Sporadic Alzheimer's disease, STZ: Streptozotocin



(157.7 ± 10.39 ; $p < 0.0001$), 55% (87.40 ± 7.50 ; $p < 0.0001$), 54% (5.52 ± 0.90 ; $p < 0.0001$), and 56% (54.92 ± 6.25 ; $p < 0.0001$), respectively, as compared to the SAD group.

Effect of PD98059& Limettin on Hippocampal *p*-tau in in SAD Mice Model

The control mice (Fig. 6A), PD98059 group (Fig. 6B), and limettin group (Fig. 6C) showed null *p*-tau expression in the brain tissue. Upregulated immunohistochemical expression of *p*-tau in the brain tissue were detected in ICV-STZ group (Fig. 6D) to 55 folds (10.73 ± 0.70 ; $p < 0.0001$) as compared to the control group. Administration of PD98059 in STZ-induced SAD group (Fig. 6E) resulted in a reduction in the deposition of *p*-tau in brain tissue to 43% (4.70 ± 0.46 ; $p < 0.0001$), as compared to the model group. Moreover, the STZ+limettin group (Fig. 6F) showed a marked reduction in the deposition of *p*-tau in brain tissue to 26% (2.93 ± 0.21 ; $p < 0.0001$) and 62% (2.93 ± 0.21 ; $p < 0.001$) as compared to the model and STZ+PD98059 group, respectively. The immunohistochemical expression was presented as area % as shown in (Fig. 6G).

Effect of PD98059 and Limettin on Abnormalities Occurred in hippocampus Histology in SAD Mice Model

The microscopic inspection of the CA3 areas of the hippocampus in several samples showed that the samples in the control group (Fig. 7A) had ordinary hippocampal morphology, unchanged intercellular matrix, and little reactivity of glial cells in addition to unharmed, properly organized pyramidal neural networks with intact nuclear and internal cellular structure. Similarly, the PD98059 group (Fig. 7B) and limettin group (Fig. 7C) samples exhibited identical data as the control group with no unusual histological changes. On contrary, the STZ model group (Fig. 7D) showed severe neuronal loss and neuronal degenerative changes with abundant figures of hyperesophilic, shrunken pyramidal neurons with vague intracellular findings alternated with number of dispersed, undamaged cells, severe swelling in brain matrix and greater numbers of infiltration of reactive glial cells. Administration of PD98059 to STZ-induced SAD group (Fig. 7E) showed mild persistent degenerative alterations in neurons combined to higher records of seemingly intact brain cells with coexistence of penetrative reactive glial cells and minimal swelling of intrinsic neurological matrices in different layers. Moreover, limettin administration to STZ-induced SAD group (Fig. 7F) has shown considerably greater neuroprotective action compared to PD98059 with minimal intermittent few records of degenerated neurons and abundant numbers of apparent well-structured neurons,

low records of reactive glial cells infiltration. Furthermore histopathological scoring illustrating neural morphology data was shown in (Fig. 7G) neuronal damage, (Fig. 7H) brain matrix edema, and (Fig. 7I) glial cell infiltrate to display the improvement through treatments administration.

Effect of PD98059 and Limettin on Neuron Cells Viability in SAD Mice Model

The control group (Fig. 8A) as well as animals received either PD98059 (Fig. 8B) or limettin (Fig. 8C) showed no significant difference in intact neuron cells, while the mice injected by STZ (Fig. 8D) indicated a decline in intact neuron cells to 41% (18.33 ± 1.53 ; $p < 0.0001$), as compared to the control group. The STZ+PD98059- group (Fig. 8E) showed significant improvement in the intact neuron count in CA3 region to 1.9-folds (35.33 ± 1.53 ; $p < 0.0001$), as compared to the STZ receiving mice. Additionally, the STZ+limettin group (Fig. 8F) increased intact neurons to 2.2-fold (40.00 ± 2.00 ; $p < 0.0001$), as compared to the model group. These results were summarized as count /field in different experimental groups in (Fig. 8G).

Discussion

Development of SAD may occur due to the complicated interplay of the environment factors, lifestyle, and genes but ageing remains the biggest risk factor for SAD. SAD is typified by the buildup of tau protein filaments and plaques containing amyloid which is directly linked to the neurodegenerative, inflammatory, and oxidative stress processes in patients' brains (Scheltens et al. 2016). This is the first study for assessment purposes of the possible protecting impact of limettin in STZ-induced SAD in mice, beside elaborating the role of *p*-ERK1/2 and *p*-GSK-3 β / *p*-CREB/ BDNF pathway through using PD98059.

Administration of either PD98059 or limettin to STZ group improved hippocampal histopathological alterations that were deteriorated in the SAD group. Noteworthy, the treated animals displayed enhanced cognitive and memory performance in the behavioral tests reflected by improved SAP and number of arm entries in Y-maze, beside MEL, time spent in the target quadrant, and platform crossing in MWM when compared to the STZ receiving animals. Furthermore, STZ+PD98059 and STZ+limettin groups potentiated the neuroprotective arm through inhibition of the persistent activation of *p*-ERK1/2 which in turn caused upregulation of *p*-GSK-3 β (Ser9), leading to the upregulation of *p*-CREB (Ser133) and BDNF. Additionally, PD98059 and limettin treated groups suppressed neuroinflammation through lowering NF- κ B which in turn suppressed IL-6, thus reducing

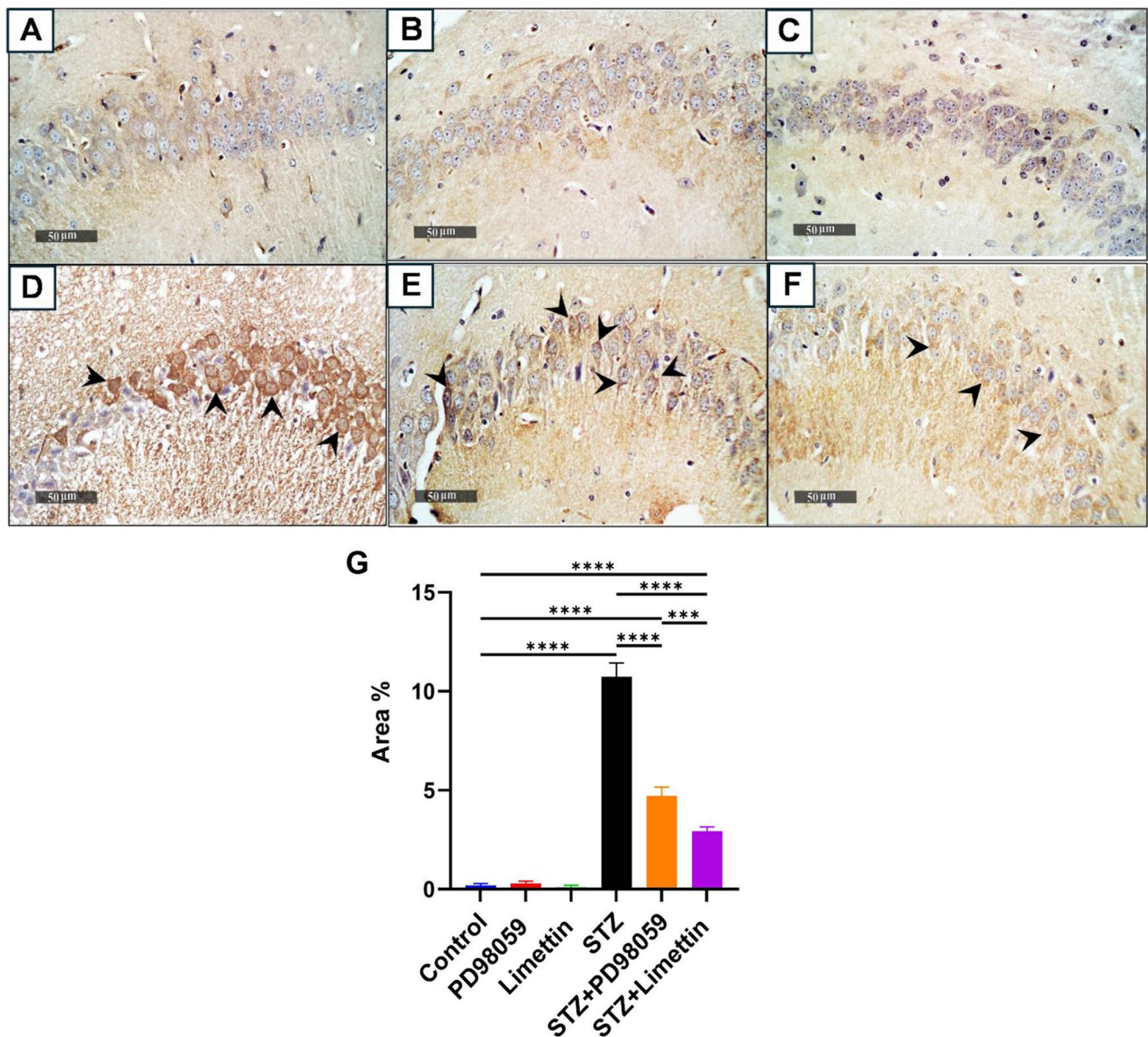


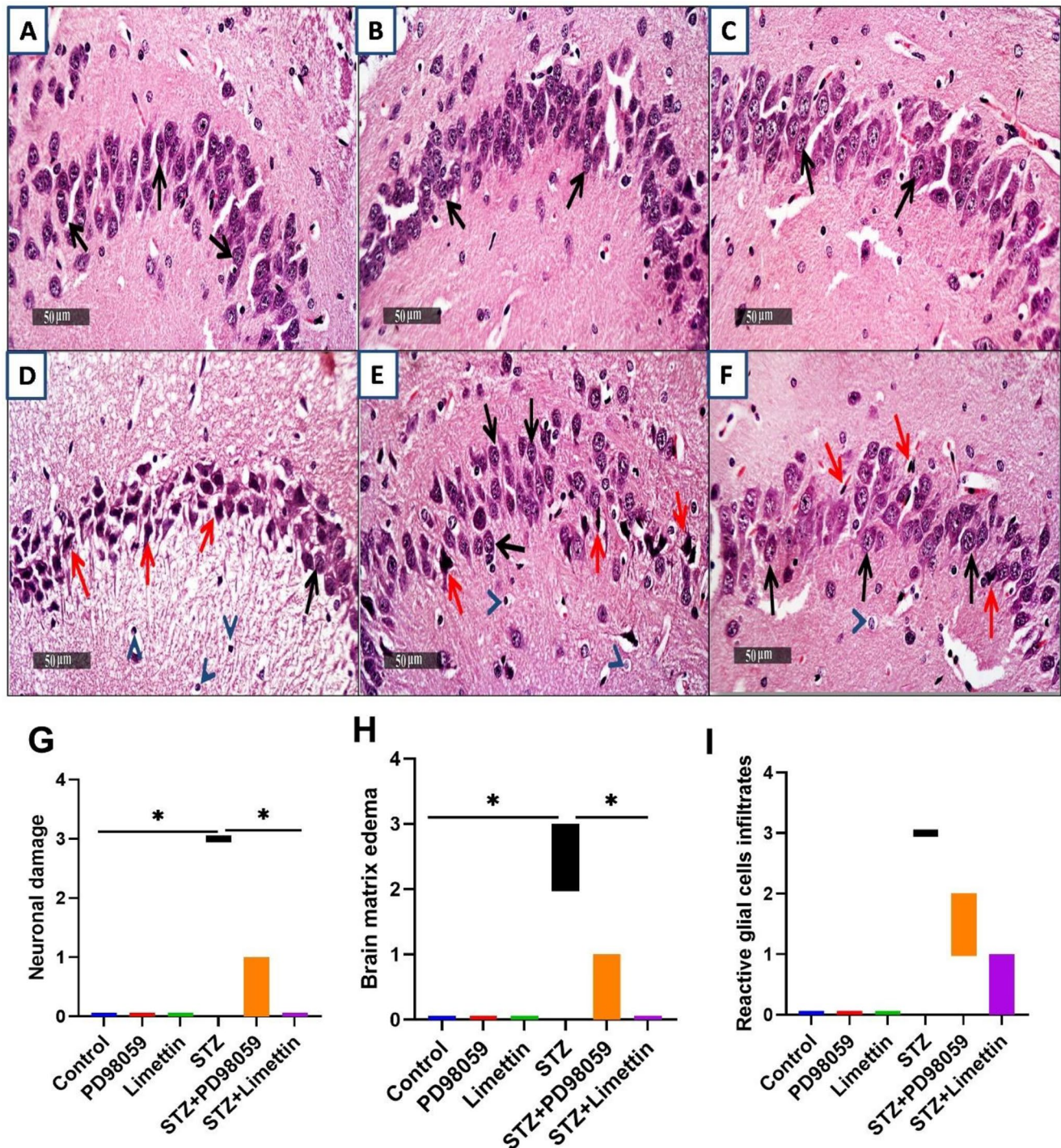
Fig. 6 Effect of limettin and PD98059 on hippocampal expression of *p*-tau in SAD mice model. PD98059 (10 mg/kg; i.p) and limettin (15 mg/kg; i.p) had been provided during a 21-day period post single ICV-STZ injection-induced SAD in mice. Sections of (A) control group, (B) PD98059, and (C) limettin groups displayed null expression of phosphorylated tau in the brain tissue, while expression of phosphorylated tau in the brain tissue was high in (D) STZ received group showed by black arrows. In (E) STZ+PD98059 group showed reduction in the deposition of phosphorylated tau in brain tissue, addi-

tionally, (F) STZ+limettin group showed marked downregulation of phosphorylated tau in brain tissue. These results were summarized as area percentage of immunohistochemical expression levels of *p*-tau in different experimental groups in (G). Data is set as mean \pm SD; ($n=3$), the asterisks (****) show statistical significance at $p<0.0001$, and (***) at $p<0.001$, tested through Tukey's multiple comparisons following One Way ANOVA. ANOVA: Analysis of variance, *p*-tau: Phosphorylated tau, SAD: Sporadic Alzheimer's disease, STZ: Streptozotocin

BACE-1 content, A β formation and downregulating *p*-tau expression, compared to the STZ group. These changes were reflected on neuronal viability observed by Toluidine blue staining.

The ICV-STZ group in the present study demonstrated a significant decline in both learning and memory processes, as evidenced by increasing MEL, a reduction in the time spent in the target quadrant, and times of platform crossing

as well in the MWM in addition to reduced SAP recorded in Y-maze test, respectively. This in comply with a study documented that STZ affected mice behaviors related to cognition and memory (Zou et al. 2017). The current study showed that STZ+PD98059 and STZ+limettin groups displayed marked improvement in memory and learning functions manifested by enhancing behavioral battery to go align with the study that discussed how ERK1/2 inhibition



by PD98059 enhanced MWM results by improving spatial memory in A β -injected rats (Ashabi et al. 2012). In addition to another study that reported ameliorating mice behaviors in lipopolysaccharide-induced memory deficit model using imperatorin, a furanocoumarin compounds that mimics limettin (Chowdhury et al. 2018).

In this work, ICV-STZ group increased the expression of *p*-ERK1/2 and downregulated *p*-GSK-3 β (Ser9), beside

reducing the hippocampal content of *p*-CREB (Ser133) and BDNF, thus participating in neuronal death and AD pathogenesis. These were in parallel with several studies that documented enhanced glomerular ERK1/2 phosphorylation in STZ-induced hyperglycemia in rats and STZ-induced SAD (Mage et al. 2002; Javadpour et al. 2021). Persistent upregulation in *p*-ERK1/2 may be involved in AD pathogenesis through its phosphorylation resulting in proliferation,

Fig. 7 Effect of PD98059 & limettin on histopathological changes and scoring in hippocampal CA3 regions in SAD mice model using (H&E) staining ($n=3$). PD98059 (10 mg/kg; i.p) and limettin (15 mg/kg; i.p) had been provided during a 21-day period post single ICV-STZ injection-induced SAD in mice. Sections of (A) control group, (B) PD98059-receiving group, as well as (C) limettin receiving group showed normal structure of different neurons in hippocampus without abnormal histological alterations. In (D) ICV-STZ injected group, severe neuronal loss and neuronal degenerative changes alternated with abundant figures of hyper-eosinophilic, shrunken pyramidal neurons with indistinct intracellular details (**red arrow**) having a small number of dispersed, seemingly undamaged cells (**black arrow**), severe edema with greater records of glial cells reactivity (**arrowhead**) were observed. In (E) STZ+PD98059 group, demonstrated mild persistent records of neuronal degenerative changes (**red arrow**) interleaved with elevated clearly visible intact neurons (**black arrow**) with coexistence of interacting penetrative glial cells (**arrow head**) and minimal edema of intercellular brain matrix in different layers, while in (F) STZ+limettin group, samples showed significant higher neurological protective effects altogether with minimal sporadic few records of degenerated cells (**red arrow**) and copious figures of apparent robust well-structured cells (**black arrow**), few persistent numbers of reactive glial cells infiltrates (**arrow head**) (50 μ m). Histopathological scoring in (G) neuronal damage, (H) brain matrix edema and (I) reactive glial infiltrates were made using the Kruskal-Wallis's test followed by Dunn's post hoc test for multiple comparison the asterisk (*) shows statistical significance at $p<0.05$. SAD: Sporadic Alzheimer's disease, STZ: Streptozotocin

activation of microglial cells, and secretion of cytokines which interfere with the role of BDNF as a neuroprotective and anti-inflammatory mediator. This in comply with previous in vivo study of spinal cord injury model as well as A β 1–42 oligomers injection in mice AD model (Morroni et al. 2016; Liang et al. 2018) and in vitro AD study utilizing Sprague Dawley rat neonatal cell cortex in cell culture (Tang et al. 2014). These results pinpoint the role of persistent stimulation of *p*-ERK1/2 with corresponding BDNF expression reduction in AD models. Likewise, another study documented reducing synaptogenesis by excessive exposure to fluoride via increasing *p*-ERK1/2, thus hippocampal BDNF downregulation in the of Sprague-Dawley rats (Chen et al. 2018). Of note, STZ+PD98059 and STZ+limettin groups reversed the previous alterations to ameliorate deterioration reported in STZ- injected mice. Furthermore, ERK1/2 phosphorylation inhibition by STZ+PD98059 group may participate in AD amelioration which may be supported by an in vitro study used hippocampal slice cultures of male Wistar rats to report that ERK1/2 activation is observed shortly following the lack of oxygen and glucose in CA1 and CA3 of hippocampus. However, the restriction of this axis by PD98059 or U0126 provided a limited level of defense towards this damage (Rundén-Pran et al. 2005). Likewise, some reported how Citrus aurantifolia oil inhibited the growth of smooth muscle cells in blood vessels through inhibition of ERK1/2 phosphorylation (Song et al. 2022) which may clarify the inhibitory effect of STZ+limettin group on ERK1/2, similarly. Another in vitro study of

melanogenesis induction in melanoma cell line showed the ERK1/2 inhibition by citropten/ limettin alone or combined with U0126, an ERK1/2 inhibitor, increased phosphorylation of CREB (Alesiani et al. 2009).

Surprisingly, ERK1/2 role in AD pathogenesis is controversial as it was documented that either activation or inhibition of ERK1/2 pathway may result in SAD progress. Herein, inhibition of ERK1/2 could halt SAD features, while some investigations revealed that ERK1/2 has positive effect on neuroplasticity, IL-10 regulation (Correa et al. 2010), hence maintaining ERK1/2 activation guards versus neuroinflammation and damage caused by A β (Ishii et al. 2016; De Araújo et al. 2022). This conflict can be resolved based on the finding that discussed how over- or under-activation of ERK1/2 may be related to AD pathogenesis. It has been found that this depends on the illness's stage/level and the brain region for example, it was reported that ERK1/2 is greater in trans-entorhinal extending neuronal axons in the early phases of neurodegeneration, while throughout the latter disease stages in neuronal cell bodies and dystrophic neurites, ERK1/2 activity is lower recommending stage-specific ERK1/2 repression occurs after ERK1/2 activation (Webster et al. 2006).

Moreover, STZ inhibited Akt, preventing GSK-3 β (Ser9) phosphorylation, which in turn increases GSK-3 β (Tyr216), leading to the hippocampal apoptosis (Moosavi et al. 2014). Noteworthy, in STZ-induced diabetes in rodents, the inhibition of *p*-CREB activity and CREB-related expression of synapse protein in hippocampus as well as decreased BDNF activity were (Liu et al. 2020; Ripoli et al. 2020). Additionally, an in vitro study showed that oil of bergamot, the source of limettin, enhanced phosphorylation of GSK-3 β at Ser9 by activation of Akt (Corasaniti et al. 2007). Also, Sustained activation of *p*-ERK1/2 leads to neuronal apoptosis via reducing *p*-GSK-3 β (Ser9) expression, this was reversed by PD98059 and limettin treatment that down-regulated *p*-ERK1/2 activation, hence increasing *p*-GSK-3 β (Ser9) expression which displays beneficial effect against A β , leading to neuroprotection (Chuang et al. 2011). Consequentially, upregulated *p*-CREB (Ser133), had an impact on memory and learning (Brightwell et al. 2005), promoted BDNF production which has a neuroprotective, neuronal cell survival, and anti-inflammatory functions to suppress neuroinflammation and tau phosphorylation as seen herein. These were in comply with those studies that showed the influence of lithium, as GSK-3 β inhibitor, on neuroblastoma SH-SY5Y human cells (Grimes and Jope 2001; Mai et al. 2002) as well as its effect in vivo and invitro in models of ischemic stroke induced excitotoxicity (Chuang et al. 2011). These studies discuss how lithium enhance phosphorylation of GSK-3 β at Ser9, thus increasing both BDNF and CREB. This goes along with an in vitro study used the

cultured neonatal ventricular myocytes in rats in ischemia/reperfusion model showed that activation of *p*-ERK1/2 for long time, *p*-GSK-3 β (Ser9) is reduced, while GSK-3 β phosphorylation/translocation of Tyr216 increased, leading to cardiac cell apoptosis (Lin et al. 2011). Altogether with another study used insulin treatment in a cloned rat pheochromocytoma cell lines showed that increase in the *p*-GSK-3 β (Ser9) levels agreed roughly with the repression in *p*-GSK-3 β (Tyr216) because insulin activate Akt, an inhibitor for ERK1/2 as well as GSK-3 β (Tyr216) (Krishnankutty et al. 2017).

Consequently, upregulated immunohistochemical *p*-tau expression and increased A β production, thus cognitive decline was noted in SAD group. On the other hand, PD98059 relieved the aforementioned alterations. These effects were in comply with this in vivo study that used ICV-A β in brain to induce AD and how U0126, as ERK1/2 inhibitor, protected against A β toxicity and tau deposition (Ashabi et al. 2012).

Regarding neuroinflammation, STZ model group showed raised NF- κ B, IL-6, and BACE-1 to add explanation of cognitive impairment occurred in this study. The presence of these inflammatory cytokines is a key characteristic of Alzheimer's disease as they are one of important causes of memory impairment (Morales et al. 2014). This could be attributed through BACE-1 activation, resulting in amyloid plaque development that promotes the pro-inflammatory reaction and creates a viscous cycle as seen in this study and documented before (Qiao et al. 2021). Administration of PD98059 and limettin to the ICV-STZ group attenuated these neuroinflammation and A β deposition via reducing NF- κ B, IL-6, and BACE-1 contents. This goes align with the restriction impact of PD98059 on IL-6, NF- κ B in an atopic dermatitis model (Yu et al. 2021), beside other studies documented the neuroprotective effect of PD98059 against BACE-1 expression in human SH-SY5Y neuroblastoma (Harrison et al. 2007) as well as A β precipitation (Rapoport and Ferreira 2000) in models of AD. Concerning STZ+limettin group, it combats against neuroinflammation and A β 40–42 aggregation to go with previous report (Kowalczyk et al. 2022b). Another in vitro study of chronic colitis model showed that earlier administration of citropiten/ limettin reduced NF- κ B and MAPK signaling pathway occurring in epithelium of intestine and triggered T cells (Lee et al. 2022b), in addition to reducing IL-6 in vascular inflammation model (Lee et al. 2022b). Also limettin and other coumarins like scoparone and umbelliferon have been reported to have antioxidant and anti-inflammatory activity showing neuroprotection (Kostova et al. 2012; Seong et al. 2019; Kowalczyk et al. 2022a; Lee et al. 2022a).

Likewise, in the current study, in addition to the biochemical changes, there are also histopathological and

immunohistochemical changes as seen in ICV-STZ injected group that showed marked decrease in intact neuron cells and increased *p*-tau deposition in align with several studies (Abdallah et al. 2021; Sirwi et al. 2021). Contrary STZ+PD98059 and STZ+limettin groups improved these changes. This neuroprotection is corroborated by additional research reported the beneficial contribution of U0126 inhibitory effect on MAPK/ERK kinase in oxidative stress model using mouse and rat neuronal cell line (Satoh et al. 2000). Noteworthy, PD98059 shielded the mitochondrial system in brain's cortex in a rat model of cardiac arrest (Zheng et al. 2020). Additionally, the potential of natural and synthetic coumarins on the CNS was documented *via* inhibiting cholinesterases and monoamine oxidase as well as microglial activation (Skalicka-Woźniak et al. 2016). Another study has shown that CA1 region of hippocampal slices in the male rats treated with 3–5 mg/kg dose of coumarin had a decline in nervous cells necrosis significantly using Nissle staining (Nasrin et al. 2021). Additionally, auraptene 25 mg/kg/day, an ingredient of many citrus fruits related to coumarines, had improved neuronal loss in hippocampus, seen by Nissle staining, in in vivo study of global ischemia mice model (Okuyama et al. 2013).

Building on earlier research, this study suggested a protective function of PD98059 and similarly limettin against SAD by targeting neuroinflammation caused by ERK1/2 as well as GSK-3 β / CREB/ BDNF pathway which contributes to AD etiology and progression.

Conclusion

PD98059 and limettin ameliorated neuroinflammation and restored cell viability associated with improved histopathological and behavioral alterations as well as restoring AD hallmarks namely, A β and *p*-tau observed in SAD-induced in mice. These effects could be mediated through suppression of persistent activation of *p*-ERK1/2 which resulted in increasing *p*-GSK-3 β (Ser9), leading to GSK-3 β inhibition causing enhancement of CREB then BDNF expressions. Hence, based on these results, PD98059 and limettin may carry hope for protecting against SAD which may be through targeting *p*-ERK1/2/*p*-GSK-3 β /*p*-CREB/BDNF pathway. Noteworthy, further studies using blocking/ inhibitory molecules to confirm neuroprotective effects through this pathway are encouraged. Moreover, further investigations are recommended to evaluate limettin activity in human subjects and its applicability as a possible treatment for SAD besides, evaluating the potential synergistic effects of PD98059 and limettin. Additionally, elaborating the conflict regarding ERK role which may vary according to the

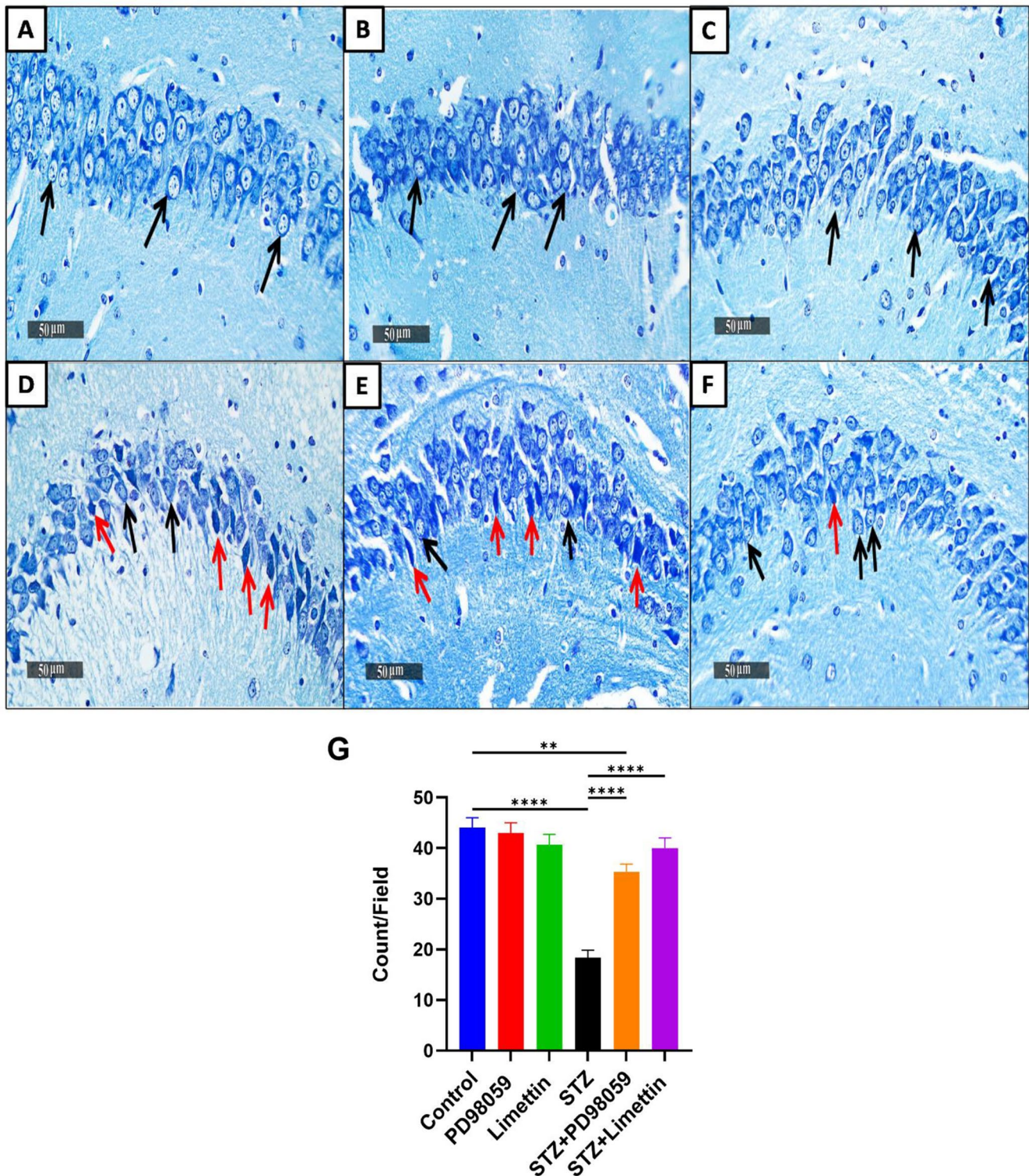


Fig. 8 Effect of PD98059 & limettin on neuron cells using Toluidine blue stain in SAD mice model. PD98059 (10 mg/kg; i.p) and limettin (15 mg/kg; i.p) had been provided during a 21-day period post single ICV-STZ injection-induced SAD in mice. The count of intact neurons was inspected in the hippocampal CA3 regions and demonstrated variance between several groups. (A) Control group, (B) PD98059, and (C) limettin groups showed no significant difference in intact neuron cells. Moreover, (D) animals injected with STZ exhibited a significant drop in intact neuronal cells, while (E) STZ+PD98059 group

displayed significant improvement in the intact neuron count in CA3 region. Similarly, (F) STZ+limettin group showed preservation of intact neurons. These results were summarized as count /field in different experimental groups in (G). **Black arrows** show intact neurons while **red arrows** show shrunken, dark degenerated neurons (50 μm). Data is set as mean±SD; (n=3), the asterisks (****) show statical significance at $p < 0.0001$ and (**) at $p < 0.01$, tested through Tukey's multiple comparisons following One Way ANOVA. ANOVA: Analysis of variance, SAD: Sporadic Alzheimer's disease, STZ: Streptozotocin

animal used, experiment duration and/or model, and cell types is suggested.

Supplementary Information The online version contains supplementary material available at <https://doi.org/10.1007/s11481-025-10211-8>.

Acknowledgements The authors are thankful to Dr. Mohamed Abdelrazik, Professor of Pathology, Faculty of Veterinary Medicine, Cairo University for his efforts in the histopathological examination, immunohistochemical staining and their data interpretation and writing.

Author Contributions R.M.: Conceptualization, Methodology, Formal analysis, Investigation, Writing– review & editing, Writing– original draft. N.S.: Conceptualization, Methodology, Formal analysis, Investigation, Writing– review & editing. N. A.: Conceptualization, Methodology, Formal analysis, Investigation, Writing– review & editing. S. M.: Conceptualization, Methodology, Formal analysis, Investigation, Writing– review & editing, Visualization. B.B.: Conceptualization, Formal analysis, Investigation, Writing– review & editing. K.S.: Conceptualization, Formal analysis, Investigation, Writing– review & editing.

Funding Open access funding provided by The Science, Technology & Innovation Funding Authority (STDF) in cooperation with The Egyptian Knowledge Bank (EKB).

Data Availability Data is available upon request.

Declarations

Competing Interests The authors declare no competing interests.

Open Access This article is licensed under a Creative Commons Attribution 4.0 International License, which permits use, sharing, adaptation, distribution and reproduction in any medium or format, as long as you give appropriate credit to the original author(s) and the source, provide a link to the Creative Commons licence, and indicate if changes were made. The images or other third party material in this article are included in the article's Creative Commons licence, unless indicated otherwise in a credit line to the material. If material is not included in the article's Creative Commons licence and your intended use is not permitted by statutory regulation or exceeds the permitted use, you will need to obtain permission directly from the copyright holder. To view a copy of this licence, visit <http://creativecommons.org/licenses/by/4.0/>.

References

- Abbas H, Gad HA, Khattab MA, Mansour M (2021) The tragedy of Alzheimer's disease: towards better management via resveratrol-loaded oral bilosomes. *Pharmaceutics* 13. <https://doi.org/10.3390/pharmaceutics13101635>
- Abdallah HM, El Sayed NS, Sirwi A et al (2021) Mangostanaxanthone IV ameliorates streptozotocin-induced neuro-inflammation, amyloid deposition, and Tau hyperphosphorylation via modulating PI3K/Akt/GSK-3 β pathway. *Biology (Basel)* 10. <https://doi.org/10.3390/biology10121298>
- Agrawal R, Tyagi E, Shukla R, Nath C (2008) Effect of insulin and melatonin on acetylcholinesterase activity in the brain of amnesic mice. *Behav Brain Res* 189:381–386. <https://doi.org/10.1016/j.br.2008.01.015>

- Alesiani D, Ciccon R, Mattei M et al (2009) Inhibition of Mek 1 / 2 kinase activity and stimulation of melanogenesis by 5, 7-dimethoxycoumarin treatment of melanoma cells. *Int J Oncol* 34:1727–1735. <https://doi.org/10.3892/ijo>
- Ali MY, Jannat S, Jung HA et al (2016) Anti-Alzheimer's disease potential of coumarins from *Angelica decursiva* and *Artemisia capillaris* and structure-activity analysis. *Asian Pac J Trop Med* 9:103–111. <https://doi.org/10.1016/j.apjtm.2016.01.014>
- Amaral AC, Perez-Nievas BG, Siao Tick Chong M et al (2021) Isoform-selective decrease of glycogen synthase kinase-3-beta (GSK-3 β) reduces synaptic Tau phosphorylation, transcellular spreading, and aggregation. <https://doi.org/10.1016/j.isci.2021.102058>. *iScience* 24:
- Ashabi G, Ramin M, Azizi P et al (2012) ERK and p38 inhibitors attenuate memory deficits and increase CREB phosphorylation and PGC-1 α levels in A β -injected rats. *Behav Brain Res* 232:165–173. <https://doi.org/10.1016/j.bbr.2012.04.006>
- Brightwell JJ, Smith CA, Countryman RA et al (2005) Hippocampal overexpression of mutant Creb blocks long-term, but not short-term memory for a socially transmitted food preference. *Learn Mem* 12:12–17. <https://doi.org/10.1101/lm.85005>
- Burillo J, Marqués P, Jiménez B et al (2021) Insulin resistance and diabetes mellitus in Alzheimer's disease. *Cells* 10. <https://doi.org/10.3390/cells10051236>
- Chen J, Niu Q, Xia T et al (2018) ERK1/2-mediated disruption of BDNF–TrkB signaling causes synaptic impairment contributing to fluoroide-induced developmental neurotoxicity. *Toxicology* 410:222–230. <https://doi.org/10.1016/j.tox.2018.08.009>
- Chen L, Feng P, Peng A et al (2020) Protective effects of isoquercitrin on streptozotocin-induced neurotoxicity. *J Cell Mol Med* 24:10458–10467. <https://doi.org/10.1111/jcmm.15658>
- Cherubini E, Miles R (2015) The CA3 region of the hippocampus: how is it? What is it for? how does it do it? *Front Cell Neurosci* 9:9–11. <https://doi.org/10.3389/fncel.2015.00019>
- Chowdhury AA, Gawali NB, Shinde P et al (2018) Imperatorin ameliorates lipopolysaccharide induced memory deficit by mitigating Proinflammatory cytokines, oxidative stress and modulating brain-derived neurotrophic factor. *Cytokine* 110:78–86. <https://doi.org/10.1016/j.cyto.2018.04.018>
- Chuang D-M, Wang Z, Chiu C-T (2011) GSK-3 as a target for Lithium-Induced neuroprotection against excitotoxicity in neuronal cultures and animal models of ischemic stroke. *Front Mol Neurosci* 4:1–12. <https://doi.org/10.3389/fnmol.2011.00015>
- Cognato G, de Bortolotto P, Blazina JW AR, et al (2012) Y-Maze memory task in zebrafish (*Danio rerio*): The role of glutamatergic and cholinergic systems on the acquisition and consolidation periods. *Neurobiol Learn Mem* 98:321–328. <https://doi.org/10.1016/j.nlm.2012.09.008>
- Corasaniti MT, Maiuolo J, Maida S et al (2007) Cell signaling pathways in the mechanisms of neuroprotection afforded by Bergamot essential oil against NMDA-induced cell death in vitro. *Br J Pharmacol* 151:518–529. <https://doi.org/10.1038/sj.bjp.0707237>
- Correa F, Hernangómez M, Mestre L et al (2010) Anandamide enhances IL-10 production in activated microglia by targeting CB2 receptors: roles of ERK1/2, JNK, and NF- κ B. *Glia* 58:135–147. <https://doi.org/10.1002/glia.20907>
- D'Hooge R, De Deyn PP (2001) Applications of the Morris water maze in the study of learning and memory. *Brain Res Brain Res Rev* 36:60–90. [https://doi.org/10.1016/s0165-0173\(01\)00067-4](https://doi.org/10.1016/s0165-0173(01)00067-4)
- De Araújo AB, Azul FVCS, Silva FRM et al (2022) Antineuroinflammatory effect of *Amburana cearensis* and its molecules coumarin and Amburoside A by inhibiting the MAPK signaling pathway in LPS-Activated BV-2 microglial cells. <https://doi.org/10.1155/2022/6304087>. *Oxid Med Cell Longev* 2022:
- Di Paola R, Galuppo M, Mazzon E et al (2010) PD98059, a specific MAP kinase inhibitor, attenuates multiple organ dysfunction

- syndrome/failure (MODS) induced by zymosan in mice. *Pharmacol Res* 61:175–187. <https://doi.org/10.1016/j.phrs.2009.09.008>
- Dillon C, Serrano CM, Castro D et al (2013) Behavioral symptoms related to cognitive impairment. *Neuropsychiatr Dis Treat* 9:1443–1455. <https://doi.org/10.2147/NDT.S47133>
- El Tabaa MM, Sokkar SS, Ramdan ES et al (2022) Does (–)-epigallocatechin-3-gallate protect the neurotoxicity induced by bisphenol A in vivo? *Environ Sci Pollut Res* 29:32190–32203. <https://doi.org/10.1007/s11356-021-18408-z>
- Epifano F, Pelucchini C, Curini M, Genovese S (2009) Insights on novel biologically active natural products: 7-Isopentenylcoumarin. *Nat Prod Commun* 4:1755–1760. <https://doi.org/10.1177/1934578x0900401228>
- Fang X, Yu SX, Lu Y et al (2000) Phosphorylation and inactivation of glycogen synthase kinase 3 by protein kinase A. *Proc Natl Acad Sci U S A* 97:11960–11965. <https://doi.org/10.1073/pnas.220413597>
- Folch J, Etcheto M, Busquets O et al (2018) The implication of the brain insulin receptor in late onset Alzheimer's disease dementia. *Pharmaceuticals* 11:1–16. <https://doi.org/10.3390/ph11010011>
- Fronza MG, Baldinotti R, Martins MC et al (2019) Rational design, cognition and neuropathology evaluation of QTC-4-MeObnE in a streptozotocin-induced mouse model of sporadic Alzheimer's disease. *Sci Rep* 9:1–14. <https://doi.org/10.1038/s41598-019-43532-9>
- Gargiulo S, Greco A, Gramanzini M et al (2012) Mice anesthesia, analgesia, and care, part I: anesthetic considerations in preclinical research. *ILAR J* 53. <https://doi.org/10.1093/ilar.53.1.55>
- Giese KP (2009) GSK-3: A key player in neurodegeneration and memory. *IUBMB Life* 61:516–521
- Grieb P (2016) Intracerebroventricular streptozotocin injections as a model of Alzheimer's disease: in search of a relevant mechanism. *Mol Neurobiol* 53:1741–1752. <https://doi.org/10.1007/s12035-015-9132-3>
- Grimes CA, Jope RS (2001) Creb DNA binding activity is inhibited by glycogen synthase kinase-3 β and facilitated by lithium. *J Neurochem* 78:1219–1232. <https://doi.org/10.1046/j.1471-4159.2001.00495.x>
- Harrison JF, Rinne ML, Kelley MR et al (2007) Altering DNA base excision repair: use of nuclear and mitochondrial-targeted N-methylpurine DNA glycosylase to sensitize astroglia to chemotherapeutic agents. *Glia* 55:1416–1425. <https://doi.org/10.1002/glia.20556>
- Honig LS, Barakos J, Dhadda S et al (2023) ARIA in patients treated with Lecanemab (BAN2401) in a phase 2 study in early Alzheimer's disease. *Alzheimer's Dement Transl Res Clin Interv* 9:1–12. <https://doi.org/10.1002/trc2.12377>
- Hoppe JB, Frozza L, Horn AP et al (2010) Amyloid- β neurotoxicity in organotypic culture is attenuated by melatonin: involvement of GSK-3 β , Tau and neuroinflammation. 48:230–238. <https://doi.org/10.1111/j.1600-079X.2010.00747.x>
- Ishii A, Furusho M, Dupree JL, Bansal R (2016) Strength of ERK1/2 MAPK activation determines its effect on Myelin and axonal integrity in the adult CNS. *J Neurosci* 36:6471–6487. <https://doi.org/10.1523/JNEUROSCI.0299-16.2016>
- Javadpour P, Askari S, Rashidi FS et al (2021) Imipramine alleviates memory impairment and hippocampal apoptosis in STZ-induced sporadic Alzheimer's rat model: possible contribution of MAPKs and insulin signaling. *Behav Brain Res* 408. <https://doi.org/10.1016/j.bbr.2021.113260>
- Kamat PK (2015) Streptozotocin induced Alzheimer's disease like changes and the underlying neural degeneration and regeneration mechanism. *Neural Regen Res* 10:1050–1052
- Kataria I (2021) Youth priorities for global health. *Nat Med* 27:1497. <https://doi.org/10.1038/s41591-021-01474-8>
- Kostova I, Bhatia S, Grigorov P et al (2012) Coumarins as antioxidants. *Curr Med Chem* 18:3929–3951. <https://doi.org/10.2174/092986711803414395>
- Kowalczyk J, Budzyńska B, Kurach Ł et al (2022a) Neuropsychopharmacological profiling of scoparone in mice. *Sci Rep* 12:1–13. <https://doi.org/10.1038/s41598-021-04741-3>
- Kowalczyk J, Skalicka-Wozniak K, Budzyńska B et al (2022b) Coumarin derivatives against amyloid- β 40–42 peptide and Tau protein. *Curr Issues Pharm Med Sci* 35:67–74. <https://doi.org/10.2478/cipms-2022-0013>
- Krishnankutty A, Kimura T, Saito T et al (2017) In vivo regulation of glycogen synthase kinase 3 β activity in neurons and brains. *Sci Rep* 1–15. <https://doi.org/10.1038/s41598-017-09239-5>
- Kumar A, Singh A, Ekavali (2015) A review on Alzheimer's disease pathophysiology and its management: an update. *Pharmacol Rep* 67:195–203. <https://doi.org/10.1016/j.pharep.2014.09.004>
- Lane CA, Hardy J, Schott JM (2022) 2022 Alzheimer's disease facts and figures. *Alzheimer's Dement* 18:700–789. <https://doi.org/10.1002/alz.12638>
- Lee H-S, Kim E-N, Jeong G-S (2022a) Ameliorative effect of citropten isolated from citrus aurantifolia Peel extract as a modulator of T cell and intestinal epithelial cell activity in DSS-Induced colitis. *Molecules* 27. <https://doi.org/10.3390/molecules27144633>
- Lee H-S, Kim E-N, Jeong G-S (2022b) Ameliorative effect of citropten isolated from citrus aurantifolia Peel extract as a modulator of T cell and intestinal epithelial cell activity in DSS-Induced colitis. *Molecules* 27:4633. <https://doi.org/10.3390/molecules27144633>
- Liang J, Deng G, Huang H (2018) The activation of BDNF reduced inflammation in a spinal cord injury model by TrkB/p38 MAPK signaling. *Exp Ther Med* 1688–1696. <https://doi.org/10.3892/etm.2018.7109>
- Lin CL, Tseng HC, Chen WP et al (2011) Intracellular zinc release-activated ERK-dependent GSK-3 β -p53 and Noxa-Mcl-1 signaling are both involved in cardiac ischemic-reperfusion injury. *Cell Death Differ* 18:1651–1663. <https://doi.org/10.1038/cdd.2011.80>
- Liu P, Li H, Wang Y et al (2020) Harmin ameliorates cognitive impairment by inhibiting NLRP3 inflammasome activation and enhancing the BDNF/TrkB signaling pathway in STZ-Induced diabetic rats. *Front Pharmacol* 11:1–9. <https://doi.org/10.3389/fphar.2020.00535>
- Lyketsos CG, Carrillo MC, Ryan JM et al (2011) Neuropsychiatric symptoms in Alzheimer's disease. *Alzheimer's Dement* 7:532–539. <https://doi.org/10.1016/j.jalz.2011.05.2410>
- Mage M, Pécher C, Neau E et al (2002) Induction of B1 receptors in streptozotocin diabetic rats: possible involvement in the control of hyperglycemia-induced glomerular Erk 1 and 2 phosphorylation. *Can J Physiol Pharmacol* 80:328–333. <https://doi.org/10.1139/y02-024>
- Mai L, Jope RS, Li X (2002) BDNF-mediated signal transduction is modulated by GSK3 β and mood stabilizing agents. *J Neurochem* 82:75–83. <https://doi.org/10.1046/j.1471-4159.2002.00939.x>
- Marshall T, Williams KM (1993) Bradford protein assay and the transition from an insoluble to a soluble dye complex: effects of sodium Dodecyl sulphate and other additives. *J Biochem Biophys Methods* 26:237–240. [https://doi.org/10.1016/0165-022X\(93\)90047-R](https://doi.org/10.1016/0165-022X(93)90047-R)
- Moosavi M, Zarifkar AH, Farbood Y et al (2014) Agmatine protects against intracerebroventricular streptozotocin-induced water maze memory deficit, hippocampal apoptosis and Akt/GSK3 β signaling disruption. *Eur J Pharmacol* 736:107–114. <https://doi.org/10.1016/j.ejphar.2014.03.041>
- Morales I, Guzmán-Martínez L, Cerda-Troncoso C et al (2014) Neuroinflammation in the pathogenesis of Alzheimer's disease. A rational framework for the search of novel therapeutic approaches. *Front Cell Neurosci* 8:1–9. <https://doi.org/10.3389/fncel.2014.0112>

- Morroni F, Sita G, Tarozzi A et al (2016) Early effects of A β 1–42 oligomers injection in mice: involvement of PI3K/Akt/GSK3 and MAPK/ERK1/2 pathways. *Behav Brain Res* 314:106–115. <https://doi.org/10.1016/j.bbr.2016.08.002>
- Mullins RJ, Diehl TC, Chia CW, Kapogiannis D (2017) Insulin resistance as a link between amyloid-beta and Tau pathologies in Alzheimer's disease. *Front Aging Neurosci* 9:1–16. <https://doi.org/10.3389/fnagi.2017.00118>
- Nasrin et al (2021) (2021) Effect of Tarragon Hydroalcoholic extract and Coumarin On Memory, Tissue Index and GABAA Receptor Gene Expression in The Hippocampus of Male Rats
- Nistor M, Don M, Parekh M et al (2007) Alpha- and beta-secretase activity as a function of age and beta-amyloid in down syndrome and normal brain. *Neurobiol Aging* 28:1493–1506
- Nunez J (2008) Morris water maze experiment. *J Vis Exp* 1–3. <https://doi.org/10.3791/897>
- Okuyama S, Minami S, Shimada N et al (2013) Anti-inflammatory and neuroprotective effects of Auraptene, a citrus coumarin, following cerebral global ischemia in mice. *Eur J Pharmacol* 699:118–123. <https://doi.org/10.1016/j.ejphar.2012.11.043>
- Olivares D, Deshpande K, Shi V Y, et al (2013) N-Methyl D-Aspartate (NMDA) receptor antagonists and memantine treatment for Alzheimer's disease, vascular dementia and Parkinson's disease. *Curr Alzheimer Res* 9:746–758. <https://doi.org/10.2174/156720512801322564>
- Pan MH, Lai CS, Ho CT (2010) Anti-inflammatory activity of natural dietary flavonoids. *Food Funct* 1:15–31. <https://doi.org/10.1039/c0fo00103a>
- Prieur E, Jadavji N (2019) Assessing Spatial working memory using the spontaneous alternation Y-maze test in aged male mice. *BIO-PROTOCOL* 9:1–10. <https://doi.org/10.21769/BioProtoc.3162>
- Qiao A, Li J, Hu Y et al (2021) Reduction BACE1 expression via suppressing NF- κ B mediated signaling by Tamibarotene in a mouse model of Alzheimer's disease. *IBRO Neurosci Rep* 10:153–160. <https://doi.org/10.1016/j.ibneur.2021.02.004>
- Rajasekar N, Dwivedi S, Nath C et al (2014) Protection of streptozotocin induced insulin receptor dysfunction, neuroinflammation and amyloidogenesis in astrocytes by insulin. *Neuropharmacology* 86:337–352. <https://doi.org/10.1016/j.neuropharm.2014.08.013>
- Rajkumar M, Sakthivel M, Senthilkumar K et al (2022) Galantamine tethered hydrogel as a novel therapeutic target for streptozotocin-induced Alzheimer's disease in Wistar rats. *Curr Res Pharmacol Drug Discov* 3:100100. <https://doi.org/10.1016/j.crphar.2022.10.0100>
- Rapoport M, Ferreira A (2000) PD98059 prevents neurite degeneration induced by fibrillar β -amyloid in mature hippocampal neurons. *J Neurochem* 74:125–133. <https://doi.org/10.1046/j.1471-4159.2000.0740125.x>
- Rasheed NOA, Sayed NS, El, El-khatib AS (2018) Progress in neuropsychopharmacology & biological psychiatry targeting central B 2 receptors ameliorates streptozotocin-induced neuroinflammation via Inhibition of glycogen synthase kinase3 pathway in mice. *Prog Neuropsychopharmacol Biol Psychiatry* 86:65–75. <https://doi.org/10.1016/j.pnpbp.2018.05.010>
- Rattanapornsompong K, Ngamkham J, Chavalit T, Jitrapakdee S (2019) Generation of human pyruvate carboxylase knockout cell lines using retrovirus expressing short hairpin RNA and CRISPR-Cas9 as models to study its metabolic role in Cancer research
- Ripoli C, Spinelli M, Natale F et al (2020) Glucose overload inhibits glutamatergic synaptic transmission: A novel role for CREB-Mediated regulation of synaptotagmins 2 and 4. *Front Cell Dev Biol* 8:1–13. <https://doi.org/10.3389/fcell.2020.00810>
- Rojewska E, Popiolek-Barczyk K, Kolosowska N et al (2015) PD98059 influences immune factors and enhances opioid analgesia in model of neuropathy. *PLoS ONE* 10:1–19. <https://doi.org/10.1371/journal.pone.0138583>
- Rui TY, Huang HZ, Zheng K et al (2025) Tau pathology drives Disease-Associated astrocyte reactivity in Salt-Induced neurodegeneration. *Adv Sci* 2410799:1–19. <https://doi.org/10.1002/adv.202410799>
- Rundén-Pran E, Tansø R, Haug FM et al (2005) Neuroprotective effects of inhibiting N-methyl-D-aspartate receptors, P2X receptors and the mitogen-activated protein kinase cascade: A quantitative analysis in organotypical hippocampal slice cultures subjected to oxygen and glucose deprivation. *Neuroscience* 136:795–810. <https://doi.org/10.1016/j.neuroscience.2005.08.069>
- Saria A, Prast J, Schardl A, Kummer K (2015) Reacquisition of cocaine conditioned place preference and its Inhibition by previous social interaction: neurochemical and electrophysiological correlates in the nucleus accumbens corridor. *Springerplus* 4:1–32. <https://doi.org/10.1186/2193-1801-4-S1-L2>
- Satoh T, Nakatsuka D, Watanabe Y et al (2000) Neuroprotection by MAPK/ERK kinase Inhibition with U0126 against oxidative stress in a mouse neuronal cell line and rat primary cultured cortical neurons. *Neurosci Lett* 288:163–166. [https://doi.org/10.1016/S0304-3940\(00\)01229-5](https://doi.org/10.1016/S0304-3940(00)01229-5)
- Scheltens P, Blennow K, Breteler MMB et al (2016) Alzheimer's disease. *Lancet (London England)* 388:505–517. [https://doi.org/10.1016/S0140-6736\(15\)01124-1](https://doi.org/10.1016/S0140-6736(15)01124-1)
- Schlichting ML, Zeithamova D, Preston AR (2014) CA 1 subfield contributions to memory integration and inference. *Hippocampus* 24:1248–1260. <https://doi.org/10.1002/hipo.22310>
- Seong SH, Ali MY, Jung HA, Choi JS (2019) Umbelliferone derivatives exert neuroprotective effects by inhibiting monoamine oxidase A, self-amyloid β aggregation, and lipid peroxidation. *Bioorg Chem* 92:103293. <https://doi.org/10.1016/j.bioorg.2019.103293>
- Sirwi A, Sayed NSE, Abdallah HM et al (2021) Umuhengerin neuroprotective effects in streptozotocin-induced Alzheimer's disease mouse model via targeting nrf2 and nf- κ b signaling cascades. *Antioxid* 10. <https://doi.org/10.3390/antiox10122011>
- Skalicka-Woźniak K, Orhan IE, Cordell GA et al (2016) Implication of coumarins towards central nervous system disorders. *Pharmacol Res* 103:188–203. <https://doi.org/10.1016/j.phrs.2015.11.023>
- Song B-W, Lee CY, Park J-H et al (2022) Cold-pressed oil from Citrus aurantifolia inhibits the proliferation of vascular smooth muscle cells via regulation of PI3K/MAPK signaling pathways. *Exp Ther Med* 23:21. <https://doi.org/10.3892/etm.2021.10943>
- Subramaniam S, Unsicker K (2010) ERK and cell death: ERK1/2 in neuronal death. *FEBS J* 277:22–29. <https://doi.org/10.1111/j.1742-4658.2009.07367.x>
- Tamagno E, Guglielmotto M, Monteleone D et al (2012) Transcriptional and post-transcriptional regulation of β -secretase. *IUBMB Life* 64:943–950. <https://doi.org/10.1002/iub.1099>
- Tang M, Shi S, Guo Y et al (2014) GSK-3/CREB pathway involved in the gx-50's effect on Alzheimer's disease. *Neuropharmacology* 81:256–266. <https://doi.org/10.1016/j.neuropharm.2014.02.008>
- Valenzuela CF, Morton RA (2014) Alcohol and developing neuronal circuits. *Neurobiology of alcohol dependence*, error. Elsevier, pp 111–130
- Vorhees CV, Williams MT (2006) Morris water maze: procedures for assessing Spatial and related forms of learning and memory. *Nat Protoc* 1:848–858. <https://doi.org/10.1038/nprot.2006.116>
- Wang L, Walia B, Evans J et al (2003) IL-6 induces NF- κ B activation in the intestinal epithelia. *J Immunol* 171:3194–3201. <https://doi.org/10.4049/jimmunol.171.6.3194>
- Webster B, Hansen L, Adame A et al (2006) Astroglial activation of extracellular-regulated kinase in early stages of alzheimer disease. *J Neuropathol Exp Neurol* 65:142–151. <https://doi.org/10.1097/01.jnen.0000199599.63204.6f>
- Yong LCJ (1992) The Theory and Practice of Histological Techniques

- Yu J, Wang L, Walzem RL et al (2005) Antioxidant activity of citrus limonoids, flavonoids, and coumarins. *J Agric Food Chem* 53:2009–2014. <https://doi.org/10.1021/jf0484632>
- Yu Z, Deng T, Wang P et al (2021) Ameliorative effects of total coumarins from the fructus of *Cnidium monnieri* (L.) cuss. On 2,4-dinitrochlorobenzene-induced atopic dermatitis in rats. *Phyther Res* 35:3310–3324. <https://doi.org/10.1002/ptr.7052>
- Zec RF, Burkett NR (2008) Non-pharmacological and Pharmacological treatment of the cognitive and behavioral symptoms of alzheimer disease. *NeuroRehabilitation* 23:425–438. <https://doi.org/10.3233/nre-2008-23506>
- Zhang XX, Tian Y, Wang ZT et al (2021) The epidemiology of Alzheimer's disease modifiable risk factors and prevention. *J Prev Alzheimer's Dis* 8:313–321. <https://doi.org/10.14283/jpad.2021.15>
- Zheng JH, Chen MH, Fu ZY et al (2020) PD98059 protects cerebral cortex mitochondrial structure and function at 48 h post-resuscitation in a rat model of cardiac arrest. *Drug Des Devel Ther* 14:1107–1115. <https://doi.org/10.2147/DDDT.S231980>
- Zou W, Yuan J, Tang ZJ et al (2017) Hydrogen sulfide ameliorates cognitive dysfunction in streptozotocin-induced diabetic rats: involving suppression in hippocampal Endoplasmic reticulum stress. *Oncotarget* 8:64203–64216. <https://doi.org/10.18632/oncotarget.19448>

Publisher's Note Springer Nature remains neutral with regard to jurisdictional claims in published maps and institutional affiliations.